Population Balance Modeling of the Dissolution of Polydisperse Solids: Rate Limiting Regimes

Significant errors can result in modeling dissolution processes if the polydispersity of the solid particles is ignored and the sample is treated as a collection of monodisperse spheres having the average size of the mixture. Population balance modeling provides an effective analytical means of predicting the effect of polydispersity on a wide variety of heterogeneous reaction systems including dissolution processes.

S. E. LeBlanc, H. S. Fogler
Department of Chemical Engineering
University of Michigan
Ann Arbor, MI 48109

Introduction

The dissolution of solid particles has been primarily modeled using a single particle or many particles having a uniform diameter. Most, if not all, practical dissolution processes involve solids consisting of a wide range or distribution of particle sizes. Particle size distributions also have a significant effect on other processes that are of importance to chemical engineers: crystallization (Randolph and Larson, 1971), fluidized-bed reactors (Levenspiel et al., 1968), and combustion (Dickinson and Marshall, 1968). Use of models based on a concept of average size, while simple, can lead to grievous errors in predicting the dissolution behavior, and they can be avoided through the use of the population balance method presented here. Particle growth processes (crystallization, precipitation, chemical reaction) and particle shrinkage processes (dissolution, combustion, grinding, sublimation, and attrition in a fluidized bed) are examples of the varied cases where an analysis in which polydispersity is taken into account will certainly be useful. Batch hydrometallurgical processes frequently used for the recovery of minerals from ores by dissolution are especially amenable to modeling using this population balance method.

Previous Work

While numerous works that model polydisperse systems using the concept of average size are present in the literature, relatively little work has been done on modeling the actual behavior of particle size distributions. Literature on the combustion and evaporation of sprays has dealt to some extent with the problem of modeling the effect of polydispersity on reaction behavior. The reaction of a population of drops produced by spray atomization or a population of solid particles produced by comminution or grinding may be analyzed in similar ways. The first model was developed by Probert (1946), who characterized a spray using a mean drop size calculated from the known initial size distribution. The spray behavior was then modeled with the assumption that it consisted of a collection of drops all of the mean drop size. This model, while crude, provided evidence that size distributions can play an important role in combustion behavior. The effect of particle size distribution on the kinetics of diffusion of oxygen into uranium dioxide powder was investigated by Gallagher (1964). A numerical solution of a discrete dissolution model was attempted, but this proved to be quite cumbersome due to the state of computing at that time. This method of analysis was also of limited usefulness because it could not predict shifts in the size distribution with time that occur during dissolution processes, making it applicable only to invariant particle size distributions. Dickinson and Marshall (1968) reexamined the evaporation of sprays previously modeled by Probert using an integral model of the combustion process and showed that the evaporation of a polydisperse spray could not be modeled adequately using a mean drop size. The integral model, which has been most commonly used to date, invariably leads to complicated numerical solutions and makes it difficult to predict shifts in the particle size distribution as a function of time and conversion.

Nuruzzaman et al. (1971) modeled the effect of particle size distributions on the burning of spray of droplets using the integral method. This model is interesting, but it does not include many features that are necessary for useful kinetic analyses, such as the effect of time and conversion on shifts in the particle size distribution, and the effect of particle size distribution parameters on the rate as a function of conversion.

Correspondence concerning this paper should be addressed to H. S. Fogler, who is presently with the Department of Chemical Engineering, University of Toledo.

A shrinking-core model for gas-solid reactions was analyzed in conjunction with particle size distributions by McIlvried and Massoth (1973). They determined that for certain situations the effect of particle size distribution on gas-solid reactions can be minimal, but as will be shown in this work, the effect can also be quite significant.

Ditl et al. (1976) examined the effect of polydispersity on the dissolution of potassium sulfate particles using an integral analysis. This study suffers from several simplifying assumptions that in general are not valid:

1. The particle size distribution on a number basis remained invariant with time, which is true only when a uniform particle size distribution is present, and this is seldom the case.
2. The mass transfer coefficient was taken as independent of particle diameter.

The mass transfer coefficient for dissolving particles in a slurry is in general a strong function of the particle diameter. This dependence on the particle diameter will markedly change the results of the analyses. In addition, Ditl concluded that a mixture with a higher degree of polydispersity would dissolve more rapidly than a more monodisperse mixture. More polydispersed mixtures yielded shorter dimensionless times at total dissolution. However, if the real times for total dissolution are compared, it can be shown that polydispersed mixtures do indeed dissolve more slowly than monodispersed systems of the same average size, contrary to the conclusions drawn by Ditl. This conclusion will be corrected and verified by the present investigation.

A better approach to analyzing the effect of particle size distributions on rate processes is the use of population balances. Population balance methods have been used occasionally in modeling chemical engineering systems. Hulbert and Katz (1964) were among the first to suggest their use.

Shapiro and Erickson (1957) used a form of population balance to model the combustion of sprays. Their work provided insight into the combustion process, but no experimental verification was included. A population balance approach was used by Sepulveda and Herbst (1978) to analyze a continuous leaching system. Their steady state analysis investigated the effect of cocurrent and countercurrent multistage systems and reactor residence time as opposed to the unsteady state analysis undertaken in the present work. Another more recent use of the population balance method was presented by Buevich and Yasnikov (1983) for the dissolution of polydisperse particles. They, however, make use of discrete as opposed to continuous distributions, which requires numerical solutions and thereby loses insights that can be gained through the use of standard distributions, such as Rosin-Rammler or log normal. In addition, their model only includes single-regime kinetics and does not account for a mixed regime or the possibility of passing from the mass-transfer limited regime to the surface-reaction-rate limited regime as the dissolution progresses. The use of self-preserving particle size distributions in the combustion process, distributions that retain their shape with reaction but decrease in amplitude, was examined recently by Cooper (1984). This approach requires the fitting of an infinite series of exponential distributions to the particle size data. This is a drawback since it inherently loses the familiar statistical parameters that are available to characterize and compare more common distributions (normal, log normal, Rosin-Rammler, gamma, etc.) as they shift due to reaction. Allen (1981) and Randolph and Larson (1971) both note that the log normal distribution is frequently applicable for ground particulate systems. Results based on the effect of a log normal distribution, along with the frequently used Rosin-Rammler distribution, will be presented in our current analysis.

The effect of particle size distribution on dissolution reactions has not been extensively studied. Most of the previous work on the effect of polydispersity on reaction systems is related to the combustion of sprays, and has serious limitations when applied to the dissolution of solid particles. The purpose of this current investigation is to model the effect of particle size distribution on the dissolution of solid particles in batch slurry reactors using a population balance technique with particular emphasis on the effect of

- Various distribution models
- Various distribution parameters
- The rate limiting step
- Shifting particle size distribution with reaction

Model Development for Rate-Limiting Regimes

A population balance will be used to develop a model for solid particle dissolution in a batch slurry reactor. For the basis of the model development, let the solid sample that is undergoing dissolution possess a number distribution function, $F(D, t)$, such that:

$$F(D,0)\Delta D = f(D,0)\Delta D N(0) \quad \begin{matrix}\text{Initial total number of}\\ \text{particles having sizes}\\ \text{between } D \text{ and } D+\Delta D\end{matrix} \tag{1}$$

where $N(0)$ = total number of particles at $t = 0$
and $f(D, 0)$ = initial number fraction distribution function (normalized).

Figure 1 illustrates the population balance formulation. A differential population balance on a diameter increment D to $D + \Delta D$ may be written as:

$$\underset{\substack{\text{Number of}\\ \text{particles}\\ \text{growing into}\\ D \text{ to } D+\Delta D}}{R(D)F(D,t)\big|_D} - \underset{\substack{\text{Number of}\\ \text{particles}\\ \text{growing out of}\\ D \text{ to } D+\Delta D}}{R(D)F(D,t)\big|_{D+\Delta D}} = \underset{\substack{\text{Accumulation}\\ \text{of particles in}\\ D \text{ to } D+\Delta D}}{\frac{\partial}{\partial t}[F(D,t)\Delta D]} \tag{2}$$

where $R(D)$ is the particle growth rate, dD/dt. This yields the following expression for the population balance:

$$-\frac{\partial}{\partial D}[R(D)F(D,t)] = \frac{\partial}{\partial t}[F(D,t)] \tag{3}$$

In order to proceed further with the model development, an expression for the particle growth (or shrinkage) rate must be obtained from kinetic considerations. The limiting cases of surface reaction controlling and mass transfer controlling will be examined. For particle dissolution, we may write

$$\frac{dM}{dt} = -kAC = -k\,A f(C) \tag{4}$$

where M is the mass of a particle, A is the particle surface area, and $f(c)$ is the rate law or mass transfer dependence on the solvent concentration. The parameter k may be either the surface

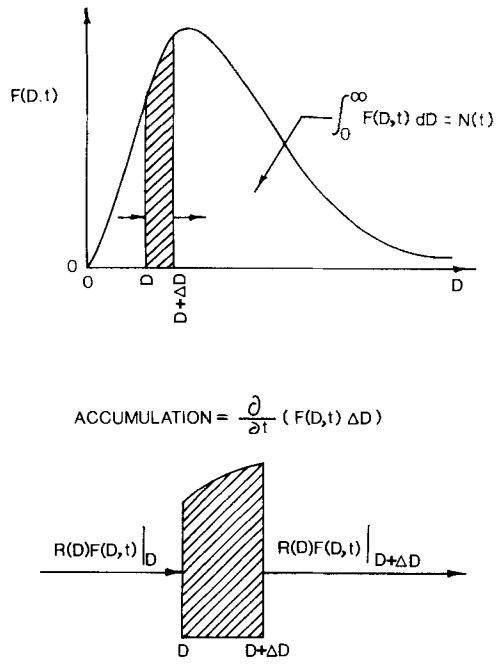

Figure 1. Population balance formulation.

reaction rate constant or the mass transfer coefficient of the solvent, depending upon which is the rate-limiting step. We now consider the two limiting cases. For small, spherical particles, which are suspended in the slurry using a high agitation rate, the slip velocity may be assumed to be negligible and the Sherwood number may be taken as two (Harriott, 1962). Therefore, the mass transfer coefficient may be expressed as

$$k = \frac{2\mathcal{D}}{D} \tag{5}$$

Equation 4 may now be rewritten for spherical particles, as

$$-\frac{dD}{dt} = \frac{4\mathcal{D}C}{\rho_s}\left(\frac{1}{D}\right) \text{ mass transfer controlling} \tag{6}$$

The chemical dependence of the rate law on the solvent can take any form, and this analysis is valid providing the solvent is present in excess so that it remains essentially constant throughout the course of the reaction: $f(c)$ = constant or c = constant.

Similarly, for surface reaction rate controlling, Eq. 4 may be written as

$$-\frac{dD}{dt} = \left(\frac{2\,k\,C}{\rho_s}\right) \text{ surface reaction controlling} \tag{7}$$

Equations 6 and 7 may now be combined into the general form

$$-\frac{dD}{dt} = \left(\frac{2KC}{\rho_s}\right) D^\beta = \alpha D^\beta = -R(D) \tag{8}$$

where α is a constant, providing there is a large excess of solvent, i.e., C is constant, and β is a constant that controls the limiting case regime as shown below:

	Mass Transfer Controlling	Surface Reaction Controlling
K	$2\mathcal{D}$	k
β	-1	0

For larger particles that do not "move" with the flow, the mass transfer coefficient may be obtained from the following correlation:

$$Sh = \frac{kD}{\mathcal{D}} = 2 + 0.6\,Re^{1/2}\,Sc^{1/3}$$

When a significant slip velocity exists (Harriott, 1962), the second term on the righthand side predominates and the mass transfer coefficient becomes:

$$k = 0.6 Re^{1/2} Sc^{1/3}\frac{\mathcal{D}}{D} = 0.6\left(\frac{\rho\bar{v}D}{\mu}\right)^{1/2} Sc^{1/3}\left(\frac{\mathcal{D}}{D}\right)$$

and the particle growth rate for this case may be placed in the same form as Eq. 8, where

$$\alpha = 0.6\,\mathcal{D}\,Sc^{1/3}\left(\frac{\rho\bar{v}}{\mu}\right)^{1/2}\left(\frac{2C}{\rho_s}\right) \text{ and } \beta = -\frac{1}{2}$$

Thus we may use $\beta = -\frac{1}{2}$ to model large mineral particles dissolving in the mass-transfer limited regime, and $\beta = -1$ for small particles.

Equation 8, which summarizes the particle growth rate, can now be used in the population balance. Substitution and simplification yields

$$\frac{\partial F(D,t)}{\partial t} - \alpha D^\beta \frac{\partial F(D,t)}{\partial D} = \alpha\beta D^{\beta-1} F(D,t) \tag{9}$$

The initial condition is the initial particle size distribution:

$$\text{I.C. } F(D,0) = f(D,0)\,N(0) \tag{10}$$

Selection of the form of the initial particle size distribution, $f(D, 0)$, is governed by the functional form that best fits the experimentally measured particle size distribution for the solids being studied. Two distribution functions commonly used for modeling ground solids are the log normal and the Rosin-Rammler (Allen, 1981).

Distribution	$f(D,0)$	
Log normal	$\frac{1}{D\ln\sigma_g\sqrt{2\pi}}\exp\left\{\frac{-\left[\ln\left(\frac{D}{Dg}\right)\right]^2}{2(\ln\sigma_g)^2}\right\}$	(11)
Rosin-Rammler	$\frac{n}{\overline{D}}\left(\frac{D}{\overline{D}}\right)^{n-1}\exp\left[-\left(\frac{D}{\overline{D}}\right)^n\right]$	(12)

The population balance model can be solved using either of these two models (LeBlanc, 1985). The details of the solution are demonstrated for for the log normal case.

Prior to solving the population balance equations we shall first dedimensionalize them using the following dimensionless parameters:

Dimensionless diameter

$$D = D/D_g \tag{13}$$

Dimensionless distribution function

$$\Phi = \frac{D\,F(D,t)}{N(0)} \tag{14}$$

Dimensionless time

$$\theta = \frac{\alpha(1-\beta)t}{(D_g)^{1-\beta}} \tag{15}$$

The physical significance of the dimensionless time may be determined from the particle growth rate expression, Eq. 8. It may easily be shown that the time required to totally dissolve a particle having an initial diameter D_g is:

$$t = \frac{D_g^{1-\beta}}{\alpha(1-\beta)} = \tau \tag{16}$$

Therefore, the dimensionless time, θ, may also be written as

$$\theta = t/\tau \tag{17}$$

The dimensionless form of the population balance is thus

$$\frac{\partial\Phi}{\partial\theta} - \frac{D^\beta}{1-\beta}\frac{\partial\Phi}{\partial D} = \frac{\beta}{1-\beta}D^{\beta-1}\Phi \tag{18}$$

and the dimensionless initial distribution function is:

Log normal
$$\Phi(D,0) = \frac{A}{D}\exp\left[-\beta(\ln D)^2\right] \tag{19}$$

where:

$$A = \frac{1}{\ln\sigma_g\sqrt{2\pi}} \qquad B = \frac{1}{2(\ln\sigma_g)^2} \tag{20}$$

The dimensionless population balance, Eq. 18, is a quasi-linear, partial differential equation that is amenable to solution using the metnod of characteristics (Hildebrand, 1976; Kovach, 1982). The ordinary differential equations that form the solution to Eq. 18, according to the method of characteristics are

$$\frac{d\Phi}{\left(\frac{\beta}{1-\beta}\right)D^{\beta-1}\Phi} = \frac{dD}{-\left(\frac{D^\beta}{1-\beta}\right)} = \frac{d\theta}{1} \tag{21}$$

Solving them provides the solution to the dimensionless population balance,

$$\Phi(D,\theta) = \frac{1}{D^\beta}H(D^{1-\beta}+\theta) \tag{22}$$

where H is an arbitrary function whose form is to be determined using the initial distribution functions. The form of H is determined by placing the initial distribution functions into the form of Eq. 22, the population balance solution, i.e.,

$$\Phi(D,0) = \frac{1}{D^\beta}H(D^{1-\beta}) \tag{23}$$

and then replacing all the $D^{1-\beta}$ terms with $(D^{1-\beta}+\theta)$. For the log normal case, the dimensionless solution is

$$\Phi = \frac{A}{D^\beta}\left(\frac{1}{D^{1-\beta}+\theta}\right)\exp\left\{-B\left[\ln\left(D^{1-\beta}+\theta\right)^{1/1-\beta}\right]^2\right\} \tag{24}$$

Important Distribution Parameters

Valuable information regarding the nature of the shifting particle size distributions can be obtained by manipulating the dimensionless solutions to the population balances. For practical batch dissolution applications, the fraction of solid dissolved, or conversion at any time is an important quantity. Let $M(t)$ represent the total mass of solid present at any time, t. Therefore, the conversion $X(t)$ is defined by

$$X(t) = 1 - \frac{M(t)}{M(0)} = 1 - \frac{\int_0^\infty D^3 F(D,t)\,dD}{\int_0^\infty D^3 F(D,0)\,dD} \tag{25}$$

or, in terms of the dimensionless quantities, D and θ:

$$X(\theta) = 1 - \frac{\int_0^\infty D^3\Phi(D,\theta)\,dD}{\int_0^\infty D^3\Phi(D,0)\,dD} \tag{26}$$

Another useful parameter in tracking the progress of the solid phase dissolution is the surface area per unit mass of the solid phase. It may also be calculated once the particle size distribution of the solid is known as a function of time. Let $S(\theta)$ represent the surface area per unit mass for the solid phase. It may easily be shown that

$$\frac{S(\theta)}{S(0)} = \frac{\int_0^\infty D^2\Phi(D,\theta)\,dD}{\int_0^\infty D^2\Phi(D,0)\,dD}\left[\frac{1}{1-X(\theta)}\right] \tag{27}$$

A third quantity that provides some useful insight into the dissolution behavior of distributions is the number fraction of solid particles remaining at any time, $N(\theta)/N(0)$.

$$\frac{N(\theta)}{N(0)} = \int_0^\infty \Phi(D,\theta)\,dD \tag{28}$$

The parameters defined in this section coupled with an analysis of the population balance solutions provide a tractable model for studying the dissolution of polydisperse solids.

Discussion of Results

The initial dimensionless log normal particle size distributions are shown in Figure 2. As σ_g approaches 1 the distribution

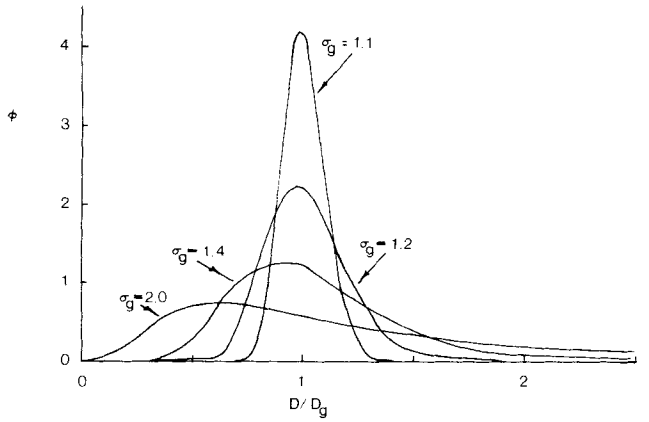

Figure 2. Initial dimensionless log normal distribution.

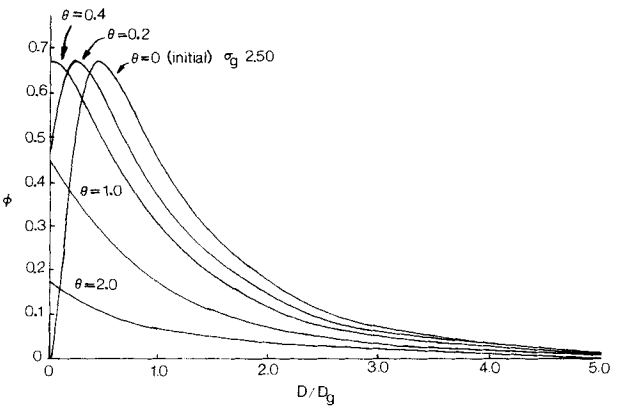

Figure 3. Log normal distribution shift, surface-reaction-rate limited case.

becomes monodispersed. These initial distributions shift as the dissolution reaction progresses. For an initial log normal distribution that is surface-reaction-rate limited ($\beta = 0$), the particle size distribution as a function of time becomes:

$$\Phi = \left(\frac{A}{D + \theta}\right) \exp\{-B[\ln(D + \theta)]^2\} \tag{29}$$

Comparison of Eq. 29 with the initial distribution given by Eq. 19 indicates that for a surface-reaction-rate limited dissolution process the distribution merely shifts laterally with dimensionless time. This behavior is illustrated in Figure 3 for an initial log normal distribution with $\sigma_g = 2.5$. Typical values for σ_g for powdered samples range between 1.3 and 3.0. The area under these curves is equal to the fraction of the initial total number of particles present at any time. Thus, the shift in a portion of the distribution past a dimensionless diameter of zero corresponds to total dissolution (or disappearance) of these particles. Notice that if the initial distribution is narrow, $\sigma_g < 1.4$ for example, the distribution can first shift to smaller diameters, while the total number of particles remains constant. The shift is a result of a loss in mass of the particles, but no particles have totally disappeared, so the area under the curve remains the same as it was initially.

For a mass-transfer limited reaction, $\beta = -1$, the dimensionless log normal solution becomes:

$$\Phi = \left(\frac{AD}{D^2 + \theta}\right) \exp\{-B[\ln(D^2 + \theta)^{1/2}]^2\} \tag{30}$$

which does not correspond to simply a lateral shift of the distribution in time. The dynamic behavior of typical log normal distributions for mass-transfer limited reactions is illustrated in Figure 4. Comparison of the mass transfer curves with the surface-reaction-rate limited curves must be done with caution. The dimensionless time θ for these two plots is not the same. From Eq. 16, θ is clearly dependent on the rate-limiting regime due to the τ dependence on α and β. These results are summarized in Table 1. Therefore, if it is desired to compare the curves for the limiting regimes, it must be done in the real-time domain as opposed to the dimensionless time domain.

The conversion vs. time behavior of these distributions is illustrated in Figure 5. An important point demonstrated by these figures is that the more polydisperse a distribution is, the longer it will take to dissolve in either rate-limiting regime. This is in direct contradiction to the conclusions of Ditl et al. (1976) who concluded that a polydisperse mixture would dissolve more rapidly than a monodisperse mixture. This erroneous conclusion was due to a misinterpretation of the dimensionless time information as described above. The dimensionless times in that analysis incorporated the polydispersity index and were thus distribution-dependent. This example proves the point that if the governing equations are dedimensionalized using different time constants, valid comparisons can only be made in the real-time domain. Another important concept illustrated by Figure 5 is the fallacy of predicting the conversion-time behavior of a polydisperse mixture using a monodispersed collection of spheres of the average diameter. For example, consider a log normal distribution having a geometric standard deviation σ_g of 2.5 and a geometric mean diameter on a number basis of 1 μm. By definition, τ is the time required to totally dissolve a particle whose initial diameter is the characteristic diameter, i.e., $D = 1$. Therefore, if we approximate our example distribution as a monodispersed collection of 1 μm dia. spheres, they should be totally dissolved (conversion = 1) at $t = \tau$, or $\theta = 1$. Calculations based on the population balance model indicate that the dissolution is essentially complete at $\theta = 5{,}000$ for a mass-transfer limited case or $\theta = 30$ for a surface-reaction-rate limited case. This shows the magnitude of the error that can be incurred using a monodispersed approximation based on number average size.

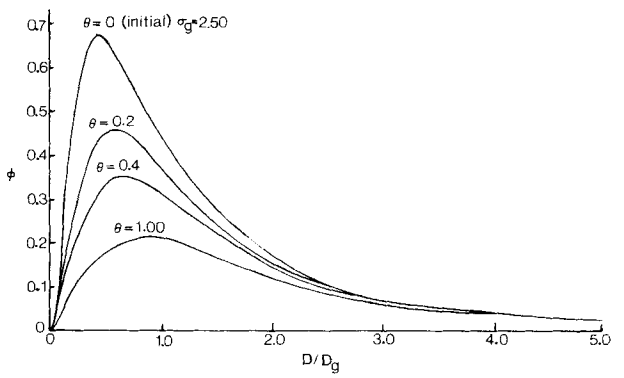

Figure 4. Log normal distribution shift, mass-transfer limited case.

Table 1. Parameter Summary for Rate-Limiting Regimes

	Mass-Transfer Limited	Surface-Reaction Limited
β	-1	0
α	$\frac{4\mathcal{D}C}{\rho_s}$	$\frac{2kf(C)}{\rho_s}$
τ	$\frac{\rho_s(D^*)^2}{8\mathcal{D}C}$	$\frac{\rho_s D^*}{2kf(C)}$

Table 2. Predicted Total Dissolution Times θ

Limiting Regime	θ: Monodispersed Approximations Based On D_{gn}	θ: Monodispersed Approximations Based On D_{gV}	θ: Polydispersed Population Balance Model
Mass Transfer	1	154	5,000
Surface Reaction rate	1	12.4	30

Perhaps a more realistic comparison is the use of a monodispersed model based on the geometric mass average diameter. For our example distribution, the geometric mass average diameter would be 12.4 μm. For a mass-transfer limited reaction of this monodispersed approximation the predicted θ for 100% conversion is 154 and for a surface-reaction-rate limited case θ = 12.4. These results are summarized for the example initial log normal distribution ($\sigma_g = 2.5, D_{gn} = 1, D_{gv} = 12.4$) in Table 2. As might be expected, a monodispersed model based on the geometric mass average diameter is a better approximation than one using the geometric number average diameter, but serious errors are still incurred. At the time for total dissolution predicted by the monodisperse approximation, the population balance model shows that the conversion should actually be 92% for the surface reaction case and 72% for the mass-transfer limited case. These errors increase as the polydispersity of the initial sample increases.

One of the most interesting results of the population balance model is that it predicts some unusual trends in dissolution phenomena that have been observed experimentally. For example, the dissolution behavior of a number of manganese oxides in hydriodic acid have been investigated (LeBlanc, 1985) and the dimensionless surface area per unit mass of these minerals is plotted as a function of conversion in Figure 6. Notice that the surface area/mass increases with conversion for MnO and MnO_2, but decreases for Mn_2O_3 (initially) and Mn_3O_4. The minimum in the plot for Mn_2O_3 is due to other complicating factors occurring during the dissolution (i.e., nonuniform surface attack and surface instabilities) and is discussed elsewhere (LeBlanc, 1985). Figures 7 and 8 show the same type of plots obtained from solutions of the population balance model. These figures indicate that the change in surface area per unit mass with conversion is dependent on the polydispersity of the initial distribution. Nearly monodispersed distributions increase their surface area per unit mass with conversion, while the area of highly polydispersed samples decreases with conversion. The curve labeled "monodispersed" in Figures 7 and 8 is a plot of the dimensionless surface area per unit mass as a function of conversion for a single particle. This result, Eq. 31, may be obtained from the single particle physical property definitions, (conversion, surface area per unit mass, etc.).

$$\frac{S(\theta)}{S(0)} = \frac{1}{[1 - x(\theta)]^{1/3}} \tag{31}$$

Notice that as the distributions approach monodispersity, (σ_g = 1), the population balance solutions approach the single particle solution for all cases. Even though the modeling was based on spherical particles, the application of this analysis is not restricted merely to spheres. For any arbitrarily shaped particle, a particle shape factor δ may be incorporated into the definition of the surface area/mass.

$$S(0)_{\text{particle}} = \delta S(0)_{\text{sphere}} \tag{32}$$

If as the dissolution progresses the shape factor remains constant, then the results of the model based on spherical particles will be applicable. The experimentally measured log normal distribution parameters for the manganese oxides previously dis-

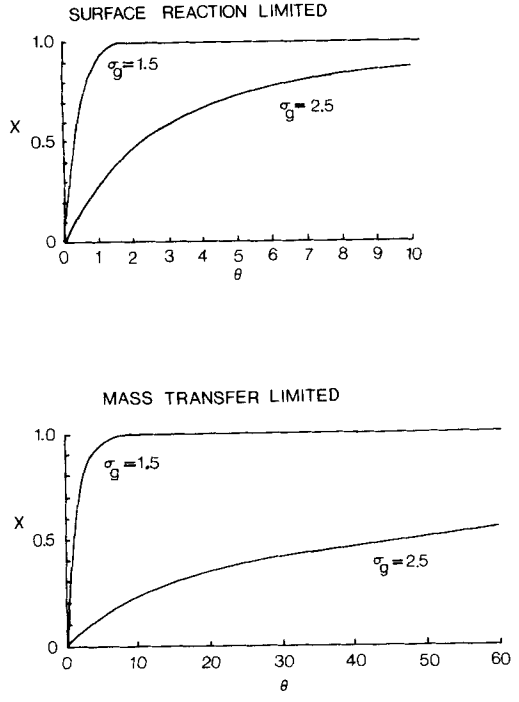

Figure 5. Log normal distribution, conversion vs. time.

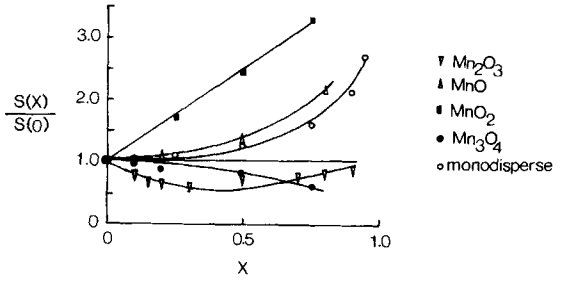

Figure 6. Dimensionless surface area/mass vs. conversion for pure manganese oxides.

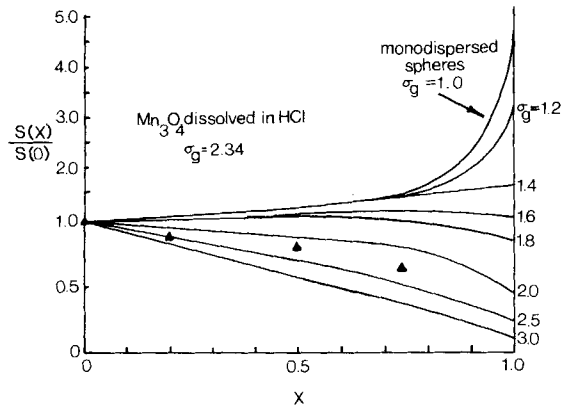

Figure 7. Log normal distribution, surface-reaction-rate limited: dimensionless area/mass vs. conversion.

cussed are summarized in Table 3. From our kinetics studies of the manganese oxides in hydriodic acid (LeBlanc, 1985), the dissolution of MnO and MnO_2 are mass-transfer limited while the dissolution of Mn_2O_3 and Mn_3O_4 are surface-reaction-rate limited. Comparing Figures 6, 7, and 8, it is easily seen that the population balance model correctly predicts the experimentally observed trends of increasing and decreasing surface areas. The data for Mn_3O_4 are replotted in Figure 9 and the agreement between the experimental data points and the population balance model is quite good. Deviations from the population balance model can be explained in terms of nonuniform particle attack and variation in the particle shape factor during the dissolution process.

The effect of large particles is shown in Figure 10. As shown previously, a value of $\beta = -1/2$ corresponds to large particles dissolving in the mass-transfer limited regime. From Figure 10, we

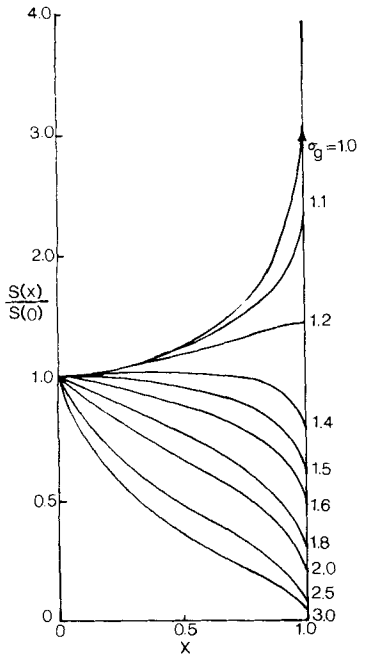

Figure 8. Log normal distribution, mass-transfer limited: dimensionless area/mass vs. conversion.

Table 3. Experimentally Determined Log Normal Distribution Parameters for Various Manganese Oxides

Oxide	D_g μm	σ_g
MnO_2	120	1.26
Mn_2O_3	10	2.58
Mn_3O_4	5.5	2.34
MnO	100	1.34

can see that the limiting cases of $\beta = 0, -1$ bound the case for large mass-transfer limited particles. The model can thus be used to predict particle dissolution behavior when a significant slip velocity exists.

Refinements of the population balance model to account for nonideal or truncated distributions and mixed-regime kinetics (LeBlanc, 1985) can also improve the usefulness and applicability of the model.

Truncated Distributions

The limiting-regime population balance model may be modified to account for the fact that actual solid samples have some minimum and maximum diameters (not 0 or ∞). In order to accomplish this, we introduce the concept of truncated distributions. Randolph and Larson give the following form for a truncated log normal distribution,

$$f(\ln D) = \frac{1}{\ln \sigma_g \sqrt{2\pi}} \cdot \exp\left(- \frac{\left\{ \ln \left[\frac{(D - D_{\min})(D_{\max} - D_{\min})}{(D_{\max} - D) D_g} \right] \right\}^2}{2 (\ln \sigma_g)^2} \right) \quad (33)$$

where this distribution is normalized as

$$\int_{D_{\min}}^{D_{\max}} f(\ln D)\, d \ln \left[\frac{(D - D_{\min})}{(D_{\max} - D)} \right] = 1$$

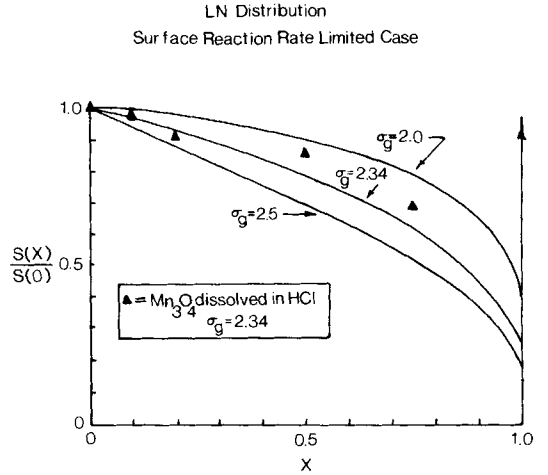

Figure 9. Dimensionless surface area per unit mass for Mn_3O_4 vs. conversion.

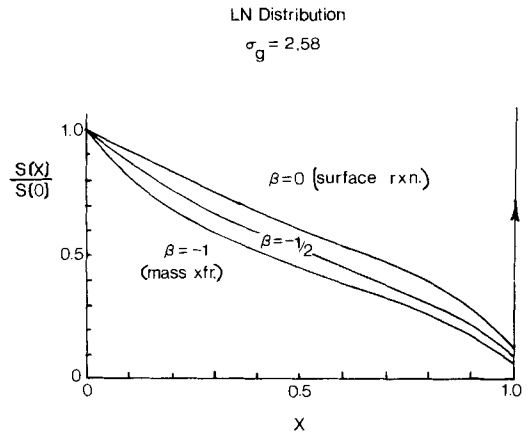

Figure 10. Effect of large particles on area vs. conversion behavior.

As $D_{min} \to 0$ and $D_{max} \to \infty$, Eq. 33 approaches the original log normal distribution. Placing Eq. 33 in another form, for use in the population balance model:

$$f(D,0) = \frac{(\ln \sigma_g\sqrt{2\pi})^{-1}(D_{max} - D_{min})}{(D - D_{min})(D_{max} - D)} \cdot \exp\left(-\frac{\left\{\ln\left[\frac{(D - D_{min})(D_{max} - D_{min})}{(D_{max} - D)D_g}\right]\right\}^2}{2(\ln \sigma_g)^2}\right) \quad (34)$$

Dedimensionalizing as before, we obtain the following dimensionless initial truncated distribution:

$$\Phi(D,0) = A\left[\frac{(D_{max} - D_{min})}{(D - D_{min})(D_{max} - D)}\right] \cdot \exp\left(-B\left\{\ln\left[\frac{(D - D_{min})(D_{max} - D_{min})}{(D_{max} - D)}\right]\right\}^2\right) \quad (35)$$

where A and B are as defined previously. Using the limiting-regime population balance cases, we impose the truncated initial distribution, Eq. 35, on the population balance solution obtained using the method of characteristics. The solution for truncated log normal distributions for limiting-regime kinetics is then,

$$\Phi(D,\theta) = \frac{A}{D^\beta}\left[\frac{D_w D_t^{z\beta}}{(D_t^z - D_{min})(D_{max} - D_t^z)}\right] \cdot \exp\left(-B\left\{\ln\left[\frac{(D_t^z - D_{min})(D_{max} - D_{min})}{(D_{max} - D_t^z)}\right]\right\}^2\right) \quad (36)$$

where the following definitions apply:

$$D_w = (D_{max} - D_{min}) = \text{breadth of initial distribution}$$

$$D_t = D^{1-\beta} + \theta$$

$$z = \frac{1}{1-\beta}$$

Important parameters for the distribution such as conversion and surface area/mass may be found as described earlier, with the modification that the limits of integration must now be D_{min} to D_{max} instead of 0 to ∞.

Discussion of Results for Truncated Distributions

As an example of the application of truncated distributions, the dissolution of Mn_2O_3 in hydriodic acid will be used. Slurry reactor studies indicate that this reaction is surface-reaction-rate limited (LeBlanc, 1985). Particle size distribution data for pure Mn_2O_3 are shown in Figure 11 on a log probability plot. Allen (1981) suggests that the best straight line be drawn through the middle of the distribution in order to determine the log normal distribution parameters. From this figure, $\sigma_g = 2.58$ and the mass geometric mean diameter is 10 microns (μm). To apply the truncated distribution analysis to this case, we must first determine D_{min} and D_{max} for the initial distribution. In Figure 11, the data points tail off at both ends of the distribution, which is characteristic of a truncated distribution. Using the method described by Orr (1983), a plot of $D/(D_{max} - D)$ for the distribution may be made for various choices of D_{max} on log probability coordinates. The D_{max} and resulting σ_g that give the best fit are then used in the truncated distribution model. The result of this procedure is shown in Figure 12 for $D_{max} = 28$ μm and $\sigma_g = 3.33$. This is a reasonable value for D_{max} because the pure material all passes through a 45 micron sieve. The minimum diameter was chosen as zero for this analysis since the data in Figure 12 do not deviate significantly from the line at small diameters. The minimum diameter can be found using the graphical method of Orr. For this system, the mineral particles after reaction were collected using a 0.45 μm filter membrane, and for a distribution this broad ($\sigma_g = 3.33$) particles less than 0.45 micron constitute a negligible fraction of the sample. The results of the truncated analysis are shown in Figure 13. Close agreement of the theory with the experimental data is obtained, with the slight remaining deviation being a consequence of the fact that the particles are nonspherical to begin with and change shape as well during the dissolution (i.e., the particles have a variable shape factor). The surface area per unit mass of spherical particles having the same distribution as the sample may be calculated from the population model. This information may be

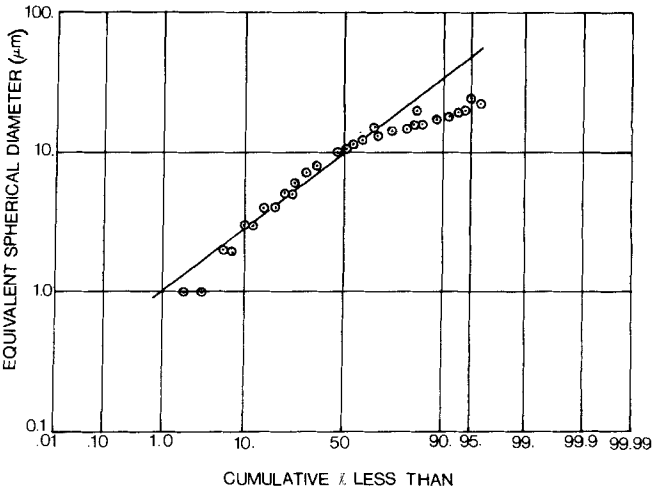

Figure 11. Log probability plot for pure Mn_2O_3.

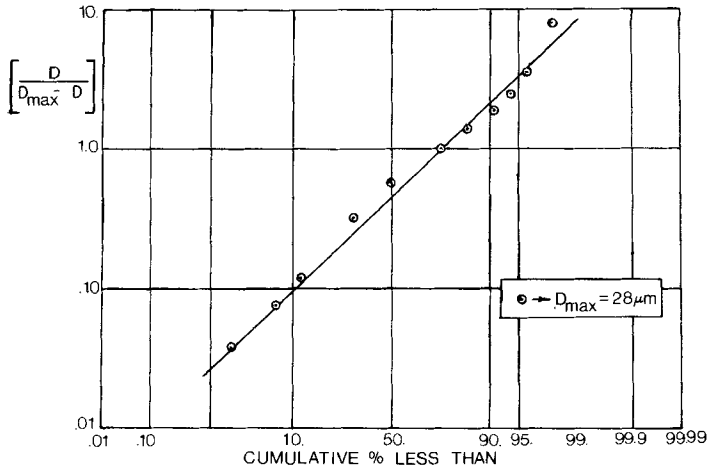

Figure 12. Determination of D_{max} for pure Mn_2O_3.

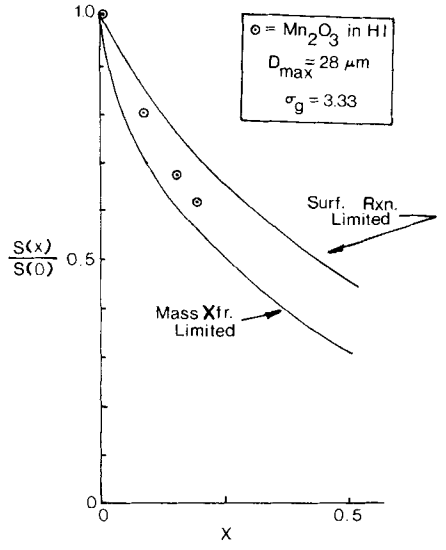

Figure 13. Effect of truncated distributions on $S(x)/S(0)$ vs. conversion.

combined with experimentally determined surface areas per unit mass for samples of Mn_2O_3 partially dissolved in HI, in order to calculate particle shape factors. The results of this analysis are shown in Table 4.

The variable shape factor indicated in Table 4 causes deviation from the population balance model, which was developed for spheres or particles that maintain a constant shape factor during dissolution. One can observe from Table 4 that the shape factor decreases with increasing conversion, indicating that the particles are smoothing initially; this is supported by scanning electron micrographs taken during the course of dissolution (LeBlanc, 1985).

Notation

A = surface area or constant in log normal distribution
B = constant in log normal equation
C = solvent concentration
D = particle diameter
$\mathcal{D}$ = diffusivity
$\boldsymbol{D}$ = dimensionless diameter
D_g = geometric mean diameter
D_{gn} = geometric number average diameter
D_{gv} = geometric volume average diameter
D_{min} = minimum particle diameter present in initial distribution
D_{max} = maximum particle diameter present in initial distribution
$D_t = \boldsymbol{D}^{1-\beta} + \theta$
$D_w = D_{max} - D_{min}$ = breadth of initial distribution
$f(c)$ = concentration dependence of surface reaction rate
$f(D, t)$ = number fraction distribution
$F(D, t)$ = number distribution at any time t
H = arbitrary solution to method of characteristics
k = mass transfer coefficient
K = constant in rate expression, $2\mathcal{D}$ or k
$M(t)$ = total mass of particles present at any time t
$N(0)$ = total number of particles present at time $t = 0$
$R(D)$ = particle growth rate
Re = Reynolds number
S = surface area/mass
Sc = Schmidt number
Sh = Sherwood number
X = conversion
$z = 1/(1-\beta)$

Greek letters

α = constant $= 2KC/\rho_s$
β = regime-controlling parameter (-1, $-\frac{1}{2}$, or 0)
Δ = increment

Table 4. Shape Factors for Dissolution of Mn_2O_3 in HI

% Conversion	$\left(\frac{\text{Surface area}}{\text{Mass}}\right)_{model}$	$\left(\frac{\text{Surface area}}{\text{Mass}}\right)_{exp}$	Shape Factor δ
0	0.209	0.721	3.45
10	0.195	0.577	2.96
15	0.188	0.492	2.61
20	0.181	0.455	2.51

δ = shape factor
ρ_s = particle density
τ = time constant
θ = dimensionless time
Φ = dimensionless number distribution
σ = geometric standard deviation

Literature cited

Allen, T., *Particle Size Measurement,* 3rd ed., Chapman and Hall, London (1981).

Buevich, Y. A., and G. P. Yasnikov, "Kinetics of Dissolution of a Polydisperse Particle System," *Teo. Khim. Tekh.*, **16**(5), 390 (1982).

Cooper, S., "The Use of Particle Size Distributions in the Modeling of Combustion Systems," *Combust. and Flame,* **56,** 279 (1984).

Dickinson, D. R., and W. R. Marshall, "The Rates of Evaporation of Sprays," *AIChE J.*, **14,** 541 (1968).

Ditl, P., J. Sestak, and K. Partyk, "Mass Transfer Kinetics in Dissolving Polydisperse Solid Materials," *Int. J. Heat Mass Trans.*, **19,** 635 (1976).

Gallagher, K. J., "The Effects of Particle Size Distributions on the Kinetics of Diffusion Reactions in Powders," *5th Int. Symp. Reactivity of Solids,* Elsevier, New York, 192 (1964).

Harriott, P., "Mass Transfer to Particles. I: Suspended in Agitated Tanks,'" *AIChE J.*, **8**(1), 93 (1962).

Hildebrand, F. B., *Advanced Calculus for Applications,* 2nd ed, Prentice Hall, Englewood Cliffs, NJ (1976).

Hulbert, H. M., and S. L. Katz, "Some Problems in Particle Technology, A Statistical Mechanical Formulation," *Chem. Eng. Sci.*, **19,** 585 (1964).

Kovach, L. D., *Advanced Engineering Mathematics,* Addison-Wesley, Reading, MA (1982).

LeBlanc, S. E., "Enhanced Mineral Dissolution," Ph.D. Thesis, Univ. Michigan (1985).

Levenspiel, O., D. Kunii, and T. Fitzgerald, "The Processing of Solids of Changing Size in Bubbling Fluidized Beds," *Powder Tech.*, **2,** 87 (1968/69).

McIlvried, H. G., and F. E. Massoth, "Effect of Particle Size Distribution on Gas-Solid Reaction Kinetics for Spherical Particles," *Ind. Eng. Chem. Fundam.*, **12**(2), 225 (1973).

Nuruzzaman, A. S. M., R. G. Sidall, and J. M. Beer, "The Use of a Simplified Mathematical Model for Prediction of Burnout of Nonuniform Sprays," *Chem. Eng. Sci.*, **26,** 1635 (1971).

Orr, C., *Encyclopedia of Emulsion Technology,* Chapter 6, P. Beecher ed. (1983).

Probert, R. P., "The Influence of Spray Particle Size and Distribution in the Combustion of Oil Droplets," *Phil. Mag.*, **37,** 94 (1946).

Randolph, A. D., and M. A. Larson, *Theory of Particulate Processes,* Academic Press, New York (1971).

Sepulveda, J. E., and J. A. Herbst, "A Population Balance Approach to the Modeling of Multistage Continuous Leaching Systems," *AIChE Symp. Ser.*, **74**(173), 41 (1978).

Shapiro, A. H., and A. J. Erickson, "On the Changing Size Spectrum of Particle Clouds Undergoing Evaporation, Combustion, or Acceleration," *ASME Trans.*, p. 775 (May, 1957).

Manuscript received June 18, 1985, and revision received May 13, 1986.